RAPID COMMUNICATIONS

PHYSICAL REVIEW B VOLUME 52, NUMBER 24 15 DECEMBER 1995-II

MBE growth and study of strain-compensated $Al_zGa_{1-z-x}In_xAs/Al_uGa_{1-u-v}In_vAs/InP$ quantum wells

H. Hillmer, R. Lösch, W. Schlapp, and H. Burkhard
Deutsche Telekom, Forschungszentrum, P.O. Box 10 00 03, 64276 Darmstadt, Germany
(Received 31 July 1995)

A series of strain-compensated $Al_zGa_{1-z-x}In_xAs/Al_uGa_{1-u-v}In_vAs/InP$ quantum-well samples have been grown by molecular-beam epitaxy and studied by low-temperature photoluminescence. In the experiment, narrow photoluminescence linewidths were obtained, mainly decreasing with growing well widths. The linewidths only reveal a weak increase with a rising number of wells. Our samples show high epitaxial quality and excellent homogeneity in the lateral and growth direction.

Strain-compensated quantum wells (QW's) are not only very interesting from the physical and epitaxial point of view but also highly attractive for applications in advanced optoelectronic and electronic devices. In recent years, QW structures including quaternary material in both wells and barriers have been grown and studied several times, using the rather well-known $Ga_xIn_{1-x}As_yP_{1-y}/Ga_zIn_{1-z}As_wP_{1-w}/InP$ material system (see, for example, Refs. 1–5). In contrast, $Al_zGa_{1-z-x}In_xAs/Al_uGa_{1-u-v}In_vAs/InP$ heterostructures have been grown and investigated rather rarely.[6–11] For this paper, we have grown, by molecular-beam epitaxy (MBE), a series of strain-compensated $Al_zGa_{1-z-x}In_xAs/Al_uGa_{1-u-v}In_vAs/InP$ QW structures having different well widths, and we will mainly report here on photoluminescence (PL) studies.

The structures were grown on semi-insulating InP by solid source MBE using two In furnaces and one furnace, respectively, for the Al, Ga, and As source materials at 515 °C substrate temperature. We avoided growth interruptions at the heterostructure interfaces leading to the border condition of correlated Al contents in the wells and the barriers for our furnace configuration. Combining x-ray-diffraction studies, low-temperature PL measurements, and corresponding simulations, we determined the well widths, barrier widths, and compositions of all layers involved, using also results from wafers with isolated bulk layers grown under nominally identical conditions. To obtain strain-compensated structures, this procedure is used to adjust the geometric and compositional parameters such as the In contents in the wells and barriers (lattice mismatch) as well as the Al contents in the wells and barriers. The geometric structure of our samples is displayed in Fig. 1. On each side of the compressively strained $Al_{0.093}Ga_{0.197}In_{0.71}As$ well having a width of L_z, a tensile strained $Al_{0.208}Ga_{0.445}In_{0.347}As$ barrier of thickness $L_B/2$ is located. This leads to a nearly complete strain compensation of the compressively strained well by two symmetrically positioned tensile strained barrier parts of widths $L_B/2$, envisaging a strain-compensated structure in which the barrier lattice mismatch times the barrier width L_B is approximately equal to the well lattice mismatch times L_z. Finally, lattice-matched $Al_{0.227}Ga_{0.243}In_{0.53}As$ layers ($\lambda_{PL} \sim 1.21$ μm) are cladding these two barrier regions asymmetrically on both sides. Table I collects the geometric and compositional parameters of our series of six samples having different well widths L_z between 0.5 and 13 nm. The excellent lateral homogeneity of the structure is confirmed by lateral x-ray-diffraction and PL scans. Figure 2 displays low-temperature PL spectra of our series of six samples showing very low linewidth. The spectral position of the peak maximum is shown to increase with decreasing L_z as displayed in Fig. 3, top. For decreasing L_z we obtain increasing quantization energies in the conduction- and valence-band QW's and, thus, increasing energies of the excitonic $1e$-hh transition (first electron subband to first heavy-hole subband), which is consistent with potential-well-model calculations. Figure 3, bottom depicts increasing PL linewidths for decreasing L_z. The PL of each sample is measured for individually selected excitation densities. The data shown in our figures were measured under conditions where a minimum PL linewidth is observed. For $L_z = 4$ nm the inset in Fig. 3, bottom shows a minimum linewidth for about 1.3 W cm^{-2} and slightly higher values below and above (due to increasing carrier concentrations and corresponding band filling).[12] These specially optimized excitation conditions show an interesting systematic behavior for our samples requiring decreasing excitation densities with increasing L_z to

50 nm	lattice-matched InAlGaAs
L_B / 2	tensile-strained InAlGaAs
L_z	compressively strained InAlGaAs
L_B / 2	tensile-strained InAlGaAs
250 nm	lattice-matched InAlGaAs
	SI - InP substrate

FIG. 1. Schematic layer design of our strain-compensated quaternary single QW samples. Shaded layers are strained.

 © 1995 The American Physical Society

TABLE I. Geometric and compositional parameters of the six samples.

	Well			Barriers			Claddings	
No.	L_z	x (In)	z (Al)	$L_B/2$	x (In)	z (Al)	x (In)	z (Al)
1	0.5	0.71	0.093	0.24	0.347	0.208	0.53	0.227
2	1.0	0.71	0.093	0.48	0.374	0.208	0.53	0.227
3	2.0	0.71	0.093	0.96	0.374	0.208	0.53	0.227
4	4.0	0.71	0.093	1.9	0.374	0.208	0.53	0.227
5	8.0	0.71	0.093	3.8	0.374	0.208	0.53	0.227
6	13	0.71	0.093	6.2	0.374	0.208	0.53	0.227

measure the respective minimum linewidths. Since the carrier capture is expected to increase with growing L_z, we believe that we generate approximately comparable carrier densities in the different single QW's of our samples under this excitation condition.[13] Note, however, that the variation of the spectral PL peak position as a function of L_z is rather similar to Fig. 3, top, if the PL experiments are performed under identical excitation densities for all samples (e.g., 1 kW/cm^2).

In the following, we try a preliminary qualitative explanation of the linewidth variation (Fig. 3, bottom) by an interplay of interface roughness (IR) and alloy disorder fluctuation (ADF) contributions. IR at the heterointerfaces of QW's leads to a lateral fluctuation of L_z and, therefore, to a lateral variation of the quantization energy. If we assume an L_z-independent microroughness of about 1 ML and lateral terrace sizes at each interface below the exciton radius, we obtain a strongly L_z-dependent IR-related linewidth broadening. The IR linewidth contribution increases for L_z, decreasing in the range from 20 nm to about 4 nm since a monolayer fluctuation causes a more and more noticeable fluctuation in L_z. However, for decreasing L_z the wave-function penetration into the barriers increases strongly. Since for very small L_z most of the wave function is located in the barriers the importance of IR is markedly disappearing, finally leading to a decrease of the IR linewidth contribution when reducing L_z from about 4 nm to nearly zero. Such a behavior was also observed for QW's in other material systems like $GaAs/Al_xGa_{1-x}As$ or $In_xGa_{1-x}As/InP$.

Our QW heterostructures contain different quaternary compositions: $Al_{0.093}Ga_{0.197}In_{0.71}As$ in the compressively strained wells, $Al_{0.208}Ga_{0.445}In_{0.347}As$ in the tensile strained barriers, and $Al_{0.227}Ga_{0.243}In_{0.53}As$ in the unstrained cladding layers. ADF is a spatial fluctuation in composition and depends on the In content x, the Al content z, and the Ga content $1-x-z$ in all three spatial directions. The ADF leads to a spatial fluctuation of the band gap and, in the bordering case of considerably growing strength, to alloy clustering. The ADF in the wells is only about 40% of the ADF amount in the barriers. The ADF of the lattice-matched $In_{0.53}Al_{0.23}Ga_{0.24}As$ cladding layers is about 92% of the ADF amount in the barriers and, thus, comparable. Since the variation of L_z will strongly vary the shape of the wave functions, the amount of the wave-function penetration into the three individual layers will vary with L_z. With decreasing L_z the wave function expands more and more into the barriers and, thus, into regions where ADF is stronger. Therefore, the linewidth broadening increases with decreasing L_z due to increasing barrier alloy disorder influence. Finally, by an interplay of IR and ADF the experimental linewidth data can be qualitatively explained.

For comparison, we also have grown a series of multiple

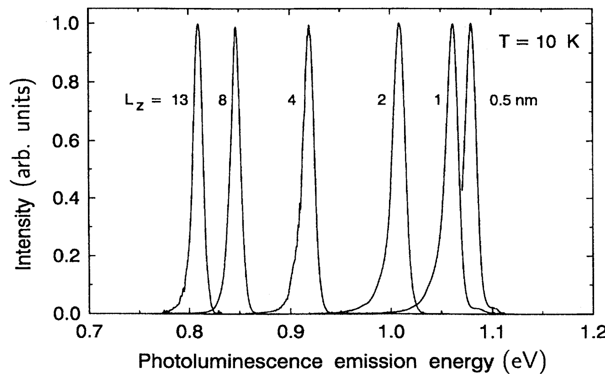

FIG. 2. Photoluminescence spectra of a set of six strain-compensated single QW samples (see Fig. 1 and Table I).

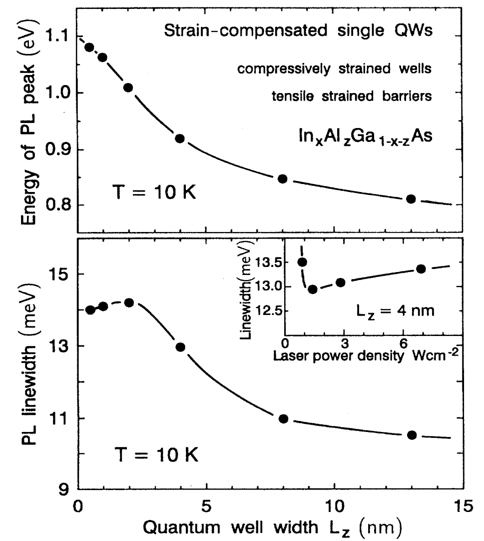

FIG. 3. Photoluminescence characterization results of the set samples. Top: energy of the maximum of the PL emission vs QW widths L_z. Bottom: corresponding PL linewidths. The six samples were measured under excitation powers providing minimum PL linewidths. For the 4-nm QW the inset shows the variation of PL linewidth with excitation power density as an example.

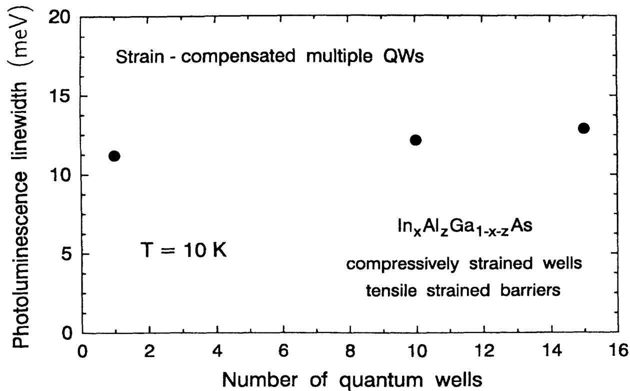

FIG. 4. Photoluminescence linewidth of strain-compensated quaternary QW structures as a funciton of the number of QW's.

QW structures of the same compositions, $L_z = 7.2$ nm and $L_B = 5.8$ nm, but with different numbers of QW's. The number of QW's is obtained by reproducing the three shaded areas in Fig. 1 as often as desired in the growth direction to obtain the envisaged number of QW's. For 10 K, Fig. 4 displays measured PL linewidths of 11.2, 12.2, and 12.9 meV, for 1, 10, and 15 QW's, respectively. We measured only a very small dependence of the linewidth on the number of QW's, demonstrating very good homogeneity in growth direction from QW to QW.

In the following, we briefly mention the advantages of strain-compensated quaternary QW structures, which can be applied, e.g., in multiple-quantum-well laser structures to improve the operation properties. In order to increase the differential gain in laser structures, the QW's, e.g., may be compressively strained ($x_{In} \sim 0.7$) to generate a light-hole-like valence band in a parallel direction and reduced electron masses. For comparison, for a desired emission wavelength close to 1.55 μm, ternary $In_{0.7}Ga_{0.3}As$ wells are fixed to a nonoptimal well width of $L_z \sim 3$ nm (for embedding QW's between $In_xAl_{1-x}Ga_yAs_{1-y}$ barriers of $\lambda_{PL} \sim 1.21$ μm). In order to overcome the disadvantage of rather narrow ternary QW's, quaternary $Al_{0.093}Ga_{0.197}In_{0.71}As$ material can be used in the wells, increasing L_z to about 7.2 nm while maintaining the desired 1.55-μm emission wavelength, since for quaternary QW's we are able to vary L_z and strain independently of each other. In addition, to provide high differential gain, the number of QW's should be sufficiently high, e.g., $\gtrsim 10$ QW's. For comparison, heterostructures including ternary $In_{0.7}Ga_{0.3}As$ QW's with $L_z \sim 3$ nm and relatively thin barriers reach the critical thickness of the total stack at about 8 QW's. In order to stabilize our structures containing $\gtrsim 10$ QW's and much wider wells ($L_z \sim 7.2$ nm), tensile strained $Al_{0.208}Ga_{0.445}In_{0.347}As$ barrier material ($L_B \sim 5.8$ nm) can be used to implement strain-compensated structures.

In summary, we have implemented and characterized strain-compensated $Al_zGa_{1-z-x}In_xAs/Al_uGa_{1-u-v}In_vAs/$ InP QW's by MBE of high epitaxial quality for the first time, to the best of our knowledge. The quaternary compressively strained wells are embedded by quaternary tensile strained barriers to realize heterostructures of almost zero net strain. Low-temperature PL shows narrow linewidths increasing with decreasing well widths. Interface roughness and alloy disorder fluctuations are discussed as possible explanations. The PL linewidths only slowly increase with a rising number of QW's, demonstrating very good vertical homogeneity.

We wish to thank A. Pöcker and H. Schwinn for x-ray diffraction, F. Steinhagen for stimulating discussions, and acknowledge the support by the European Community under Contract No. RACE 2006 Welcome.

[1]C. P. Seltzer, S. D. Perrin, M. C. Tatham, and D. M. Cooper, Electron. Lett. **27**, 1268 (1991).
[2]R. W. Glew, K. Scarrott, A. T. R. Briggs, A. D. Smith, V. A. Wilkinson, X. Zhou, and M. Silver, J. Cryst. Growth **145**, 764 (1994).
[3]L. M. Woods, P. Silvestre, P. Thiagarajan, G. A. Patrizi, and G. Y. Robinson, J. Electron. Mater. **23**, 1229 (1994).
[4]A. Hamoudi, A. Ougazzaden, Ph. Krauz, E. V. K. Rao, M. Juhel, and H. Thibierge, Appl. Phys. Lett. **66**, 718 (1995).
[5]E. Kuphal, H. Burkhard, and A. Pöcker, Jpn. J. Appl. Phys. **34**, 3486 (1995).
[6]W.-Y. Choi and C. G. Fonstad, J. Cryst. Growth **127**, 555 (1993).
[7]Ch. Zah, R. Bhat, B. N. Pathak, F. Favire, W. Lin, M. C. Wang, N. C. Andreadakis, D. M. Hwang, M. A. Koza, T.-P. Lee, Z. Wang, D. Darby, D. Flanders, and J. J. Hiesh, IEEE J. Quantum Electron. **30**, 511 (1994).
[8]H. Hillmer, R. Lösch, and W. Schlapp, J. Appl. Phys. **77**, 5440 (1995).
[9]F. Steinhagen, H. Hillmer, R. Lösch, W. Schlapp, H. Walter, R. Göbel, E. Kuphal, H. L. Hartnagel, and H. Burkhard, Electron. Lett. **31**, 274 (1995).
[10]H. Hillmer, R. Lösch, F. Steinhagen, W. Schlapp, A. Pöcker, and H. Burkhard, Electron. Lett. **31**, 1346 (1995).
[11]M. C. Wang, W. Lin, T. T. Shi, and Y. K. Tu, Electron. Lett. **31**, 1584 (1995).
[12]In our measurements the temporal average power is maintained constant for different excitation powers by appropriate duty cycles in the experiment using asymmetric chopping of the excitation light. Thus, carrier heating is negligible for all the PL spectra.
[13]A detailed analysis is started including experimental data of the variation of the QW and barrier PL intensities as a function of the well widths (barrier widths). A system of rate equations is applied including L_z-dependent lifetimes, relaxation times, capture times, and transport times.

50 nm	lattice-matched InAlGaAs
L_B / 2	tensile-strained InAlGaAs
L_z	compressively strained InAlGaAs
L_B / 2	tensile-strained InAlGaAs
250 nm	lattice-matched InAlGaAs
SI - InP substrate	

FIG. 1. Schematic layer design of our strain-compensated quaternary single QW samples. Shaded layers are strained.